NRL Report 6504

Potentiostatic Current-Potential Measurements on a Platinum Electrode in a High-Purity Closed System

S. Schuldiner, T. B. Warner, and B. J. Piersma

Electrochemistry Branch
Chemistry Division

March 6, 1967

NAVAL RESEARCH LABORATORY
Washington, D.C.

DISTRIBUTION OF THIS DOCUMENT IS UNLIMITED

CONTENTS

Abstract	ii
Problem Status	ii
Authorization	ii
INTRODUCTION	1
EXPERIMENTAL APPARATUS AND CONSIDERATIONS	1
RESULTS AND DISCUSSION	2
Cathodic Reactions	4
Anodic Reactions	5
Impurity Levels in Solution	7
CONCLUSIONS	13
REFERENCES	14

ABSTRACT

In a high-purity, closed, electrochemical system, voltage regions at which very slow reactions are rate-controlling, were accurately separated and measured. In the potential range from 0.06 to 0.13 volt, the rate-controlling step is $Pt\text{-}H + H^+ + e = H_2$ under conditions of rapid stirring with helium. A second region between 0.30 and 0.46 volt indicated a slow hydrogen-ion discharge. In the anodic range from 0.46 to > 2 volts, four distinct regions were found: a region in which oxidizable impurities reacted; a region at which water was probably oxidized to give chemisorbed OH; a region in which chemisorbed and dermasorbed O was formed; and a region in which O_2 was generated.

Maximum oxidizable and reducible impurity levels were quantitatively determined both in solution and as adsorbed species on the working electrode surface. It is shown that the impurity levels were very low. Very small additions of hydrogen or oxygen in the critical transition region (net cathodic to anodic reactions) did not appear to have catalytic effects. However, at oxygen partial pressures above 10^{-7} atm, a poisoning effect was apparent.

PROBLEM STATUS

This is an interim report on one phase of the problem of electrode mechanisms; additional work on this problem is continuing.

AUTHORIZATION

NRL Problem C05-13
Project RR 001-01-43-4754

Manuscript submitted November 2, 1966.

POTENTIOSTATIC CURRENT-POTENTIAL MEASUREMENTS ON A PLATINUM ELECTRODE IN A HIGH-PURITY CLOSED SYSTEM

INTRODUCTION

Recent work at this Laboratory (1) has shown that gas-tight, closed, electrochemical systems can be devised which will maintain a high degree of solution purity and electrode cleanliness over long periods of time. By maintaining such low levels of impurities it is possible to study reaction mechanisms in the so-called passive regions where reaction rates are so low that trace impurities could easily dominate the potential-current relationships. In order to demonstrate the feasibility of such studies and to explore the reaction mechanisms in the potential region from the gaseous hydrogen to the gaseous oxygen reaction, a potentiostatic investigation of the platinum electrode in 1M H_2SO_4 was undertaken.

EXPERIMENTAL APPARATUS AND CONSIDERATIONS

The closed electrochemical system, continuously purged with highly purified helium containing less than 1 part in 10^9 O_2, was essentially the same as previously reported (1). It consisted of a gas-tight, glass-pipe system mounted inside an N_2-filled controlled environment box. The main compartment of the cell contained a large Pt gauze electrode (~100 cm^2), a large tightly rolled cylinder of Pt gauze platinized in lead-free platinic acid (geometric area of about 30 cm^2), a Pt wire 5 cm long and 0.064 cm in diameter, and a Pt bead (at the end of a short length of exposed Pt wire) electrode with a true area (2) of 0.190 cm^2. All Pt was 99.99 percent pure; the beads were formed by melting the end of Pt wire with a hydrogen/oxygen flame. The side arm of the cell (1,3) contained both a miniature glass electrode and an αPd-H spiral wire electrode which was initially charged with enough hydrogen so that its potential was 75 mV positive to an NHE (normal hydrogen electrode). This αPd-H electrode contains less hydrogen, and its potential is positive to the maximum αPd-H electrode (4). The glass electrode was +0.585±0.005 V relative to NHE. The αPd-H electrode was the reference used to maintain potentiostatic control of the working electrode (Pt bead). The potential of this αPd-H reference was repeatedly checked against the glass electrode during the course of the investigation. The long-term changes in potential difference were ±5 mV, which is attributed to changes in the glass electrode; short-term changes were below the detectable limit of 0.001 V.

Potentiostatic control between the αPd-H reference and the Pt bead working electrode was maintained with a Wenking 61R Potentiostat, using the Pt gauze roll as the counter electrode. The potential between the Pt bead and glass electrode was monitored with a Keithley 610B Electrometer. Current flow between the Pt bead working electrode and the Pt gauze roll counterelectrode was measured with a battery-operated Keithley 601 Electrometer and recorded on a Varian G-11A recorder. Necessary precautions were taken and checks made to avoid spurious microcurrents. Such spurious or background currents were about 10^{-13} ampere.

Note: B.J. Piersma performed the work at NRL as a National Academy of Sciences Postdoctoral Resident Research Associate. Present address: Eastern Baptist College, St. Davids, Pennsylvania.

In the experimental arrangement used, with counter and working electrodes in the same compartment, part of the product generated at the counterelectrode might diffuse to the working electrode and yield an erroneously high current reading. A simple analysis shows that if the fraction K of the material generated at the counterelectrode that reaches the working electrode is less than 1.0, then an unstable positive feedback condition cannot result. If K is ~ 0.1, then the current would be ~ 11 percent high. In our case, which a tiny working electrode far removed from the counterelectrode in a solution stirred with inert gas, K was estimated to be much less than 0.1, with a correspondingly lower current error. The validity of this estimate was checked by taking additional data in a two-compartment cell in which the counterelectrode was separated from the working electrode by a glass frit, both compartments being continuously purged with He. These data agreed with the single-compartment data. Further, using the simple cell (3), several regions which showed the absence of stirring effects (Fig. 2b) demonstrated the absence of significant cross-diffusion of reactants on the measured currents.

After calibrating the glass electrode against the several Pt/H_2 electrodes, the run was started by stopping the H_2 flow into the cell. This hydrogen line was purged with helium, while being baked, for several hours. The line was then completely disconnected from the system. The environment box was then sealed and filled with N_2. The entire gas purification system and cell were continuously purged with pure helium at a flow rate of about 40 ml/min. For about one month, potential settings which ranged from 0.96 to 1.5 volts were applied to the Pt bead, wire, and gauze electrodes. After this treatment, only the Pt bead was potentiostated at various potentials in the same range for about another month. At this time, potential-current-density measurements in the very low current density regions settled down and reproducible results were obtained. In the two-month purification period the residual amounts of hydrogen and organic impurities were undoubtedly reduced to such a low value that erratic steady-state measurements were no longer obtained.

Normally, applied potentials on the working electrode were changed in such a way that current reversal was avoided. This was to approximate as closely as possible normal slow changes of species at, on, or in the working electrode. In all cases, a given potential was applied to the working electrode long enough so that a steady-state current density was achieved. The required time was strongly dependent on current density at very low current densities. This took a number of days. A current was considered steady-state if there was no monotonic trend in its mean value between successive time periods. Experimental runs up and down the entire potential span were made. In addition, increasing and decreasing potentials were applied in individual Tafel regions. Working-electrode cleanliness tests (5), based on anodic charging curve linearity in the O_{ad} regions, showed the absence of detectable amounts of impurities. The operating temperature of the cell was $26 \pm 2°C$. The oxygen content of the environment box normally was about 0.05 percent.

RESULTS AND DISCUSSION

The applied potential vs steady-state current density relations are shown in Figs. 1 and 2. The data in Fig. 1 was taken under rapid stirring conditions (350+ ml/min flow of helium) so that mass transport to and away from the electrode is maximized and the data largely represents kinetic current densities at the applied potentials E. The data in Fig. 2(a) were obtained at a He flow of 40 ml/min, and Fig. 2(b) was obtained at each applied potential by subtracting current densities i_{40} obtained at slow helium flow rates from the current densities i_{350} at fast helium flow rates. Steady-state currents at the slower He flow rate were always smaller or equal to those found at faster He flow. Therefore, the data ($\Delta i = i_{350} - i_{40}$) in Fig. 2(b) represents the increased current densities due to increased diffusion rates at each applied potential.

Because of the very low current densities obtained in the potential span studied, it is obvious that net surface processes are relatively slow so that the method used for separation of surface kinetic from solution diffusion-controlled currents is accurate. In all

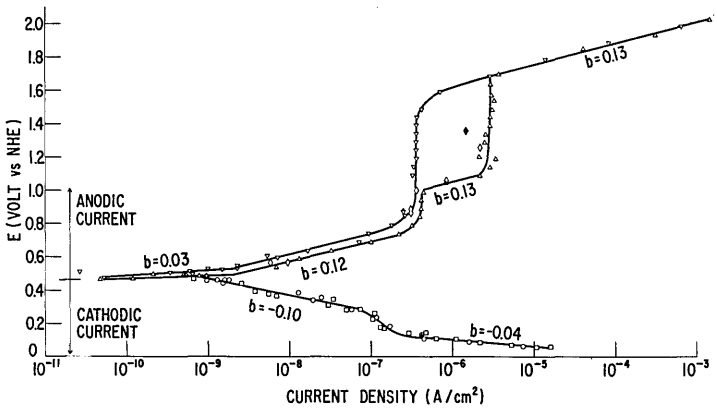

Fig. 1 - Potentiostatic current density vs applied potential E on Pt electrodes for a helium flow rate of 350 ml/min. Curves are labeled: o cathodic current, increasing applied potentials; □ cathodic current, decreasing applied potentials; △ anodic current, increasing applied potentials; ▽ anodic current, decreasing applied potentials; ◊ anodic current, intermediary reversal of applied potential values; and ♦ taken under special conditions (see text).

cases (except where trace impurities are the primary reactants) the amounts of reactant (hydrogen ion or water) are present in large quantities. Therefore, the diffusion of these reactants to the surface will not be rate-controlling. In the cases where diffusion of very small amounts of products away from the surface occurs, such mass transport phenomena could affect the currents measured. However, even in these cases, surface processes must be slow and are to a large degree controlling.

Cathodic Reactions

The data in Figs. 1 and 2 show two distinct cathodic current regions (which were independent of successively increasing or decreasing potential settings) in the potential range from 0.06 to 0.46 volt. From 0.06 to 0.13 volt, Fig. 1 shows a Tafel slope b of -0.04, whereas Fig. 2(a) shows a slope of -0.035 and Fig. 2(b) a slope of -0.03. Since the data in Fig. 2(b) is the current density difference between rapidly and slowly stirred solution, increased diffusion of small amounts of products away from the surface is indicated, and the increase in current density is primarily due to this diffusion. The -0.03 slope undoubtedly indicates that the diffusion of molecular hydrogen away from the electrode surface into solution is rate-controlling. Hence the Knorr (6,7) mechanism is rate-controlling. On the other hand, the -0.04 slope shown in Fig. 1 confirms and extends the previous work of Schuldiner (8) who showed that, when vigorously stirring with an inert gas, the rate-controlling step for the hydrogen formation reaction at very low active H

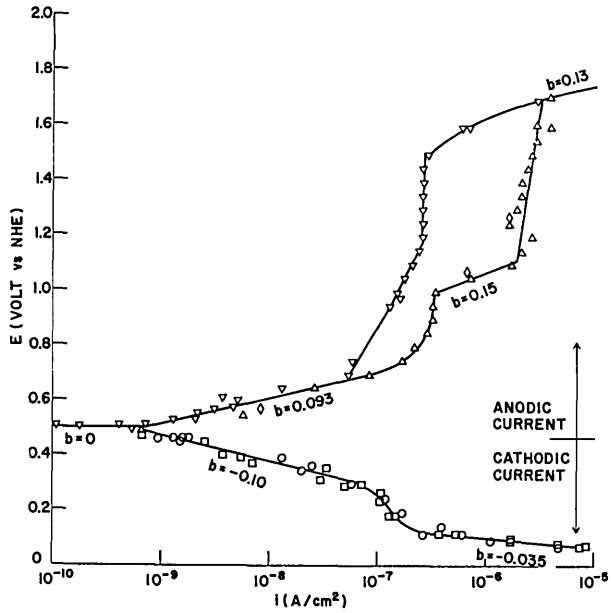

(a)

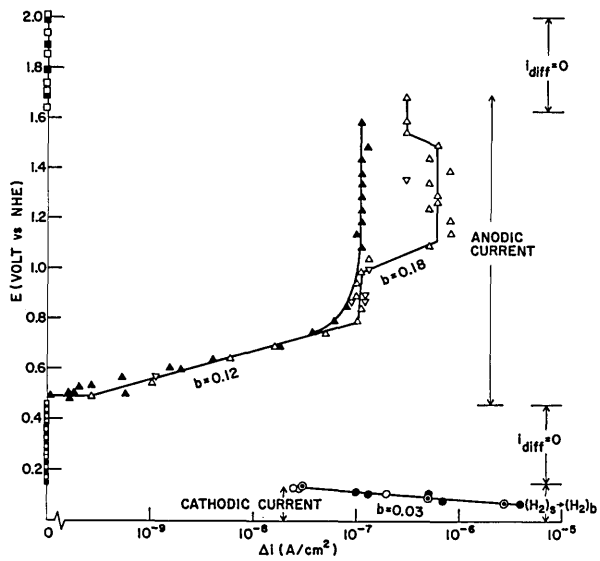

(b)

Fig. 2 - (a) Potentiostatic current density i vs potential E on Pt electrodes for a helium flow rate of 40 ml/min (symbols are the same as in Fig. 1), and (b) current density difference Δi between helium flow rate at 350 ml/min and 40 ml/min vs potential E. Figure 2(b) curves are labeled: o cathodic current, increasing applied potentials; ● cathodic current, decreasing applied potentials; △ anodic current, increasing applied potentials; ▲ anodic current, decreasing applied potentials; ▽ anodic current, intermediate reversal of applied potentials; □ Δi = O, increasing applied potentials; and ■ Δi = O, decreasing applied potentials.

coverages changes from combination of adsorbed H_{ad} atoms to electrochemical desorption of H_{ad} atoms ($H^+ + H_{ad} + e = H_2$). In that work (8) a slope of -0.04 was obtained on Pt at potentials more anodic than 0.02 volt. In Fig. 1, the minimum potential is 0.06 volt. The intermediate slope of -0.035 shown in Fig. 2(a) indicates mixed kinetic and diffusion control.

Following a transition region from 0.13 to 0.30 volt, Fig. 1 shows another Tafel slope of -0.10 which ranges from 0.30 to 0.46 volt. Fig. 2(b) shows that in the entire potential range from 0.13 to 0.46 volt there is no diffusion-limiting component. Hence, a reasonable assumption is that in this potential range the Tafel slope of -0.10 indicates a slow discharge of H^+ to H as the rate-controlling step. Evidently, under these potential conditions the surface coverage with H_{ad} atoms is so low that the electrochemical desorption mechanism is negligible and the energetics of the surface is such that slow discharge may be controlling. The amounts of H_{ad} formed in this region are so low that only a few monolayers would be involved over the several days in which the measurements were taken.

This is an interesting finding inasmuch as Horiuti and Polyani (9) concluded that as the heat of adsorption of H atoms increases, the rate of the discharge step would increase. Parsons (10) and Gerischer (11), however, showed that after a critical free energy of adsorption of H atoms is reached, the rate of the discharge step decreases. Our results at these very low coverages confirm the Parsons and Gerischer treatment. An examination of their rate equations for the case of very low surface coverage with H atoms and essentially zero H_2 partial pressure favors the possibility of H^+ discharge being rate-controlling under the given conditions. Slow surface diffusion or absorption or desorption steps which would be unaffected by solution stirring rates are possible also, but it is not obvious how these steps would give a Tafel slope of -0.10.

One of the most important aspects of the lack of dependence on the solution stirring rate in the 0.13- to 0.46-volt range is that this shows that the impurity level of reducible substances in our solution must be below a level to give current densities of about 10^{-9} A/cm^2. More will be said about reactable solution impurities in a later section.

In the vicinity of 0.46 volt there is a shift from a net cathodic to a net anodic reaction. In principle, in the total absence of reactive trace impurities and with sensitive enough potential control, one should find a potential at which zero current flows. This, of course, is a virtually impossible experimental condition to reach. However, the minimum current density reached in the transition from cathodic to anodic does give an indication of solution purity. Another important conclusion which can be reached is that at about 0.46 volt, the electrode is virtually completely free of sorbed hydrogen and oxygen. In the course of our experiments, after the Pt bead electrode was potentiostatically kept in the vicinity of 0.46 volt for many days, the open-circuit potential on this electrode was very close to 0.48 volt. This further indicates that a Pt electrode free of both hydrogen and oxygen will have a potential close to 0.46 volt. In other words, the open-circuit rest potential of pure Pt in a helium-saturated 1M H_2SO_4 solution is about 0.46 volt vs NHE. The presence of dermasorbed* H lowers that potential. Dermasorbed H can control the open-circuit potential down to as low as 0.18 volt (1).

Anodic Reactions

On the anodic side of the curves shown in Fig. 1, four distinct Tafel regions are obvious. One should further note that there are hysteresis effects, except in the potential region above 1.7 volts. The reason for this hysteresis is most likely due to the dermasorption of atomic oxygen in the Pt skin which takes place at potentials above 1.4 volt. This always gave

*From "derma"—beneath the skin—and "adsorption." Dermasorption refers to a kind of selective absorption of gas atoms into a relatively few atomic layers of metal immediately below the surface atomic layer.

lower current densities at a given applied potential. Changing the potential in either a more positive or more negative direction before this voltage is reached does not affect the current-density potential relation. However, once a 1.4-volt potential is exceeded, hysteresis occurs.

The potential region with the Tafel slope of 0.03 is most likely due to impurities in solution. The diffusion-limiting overvoltage was undoubtedly a factor. This would indicate that oxidizable impurities, such as hydrogen and organic species, are present to an amount which can give a maximum current density of about 2×10^{-9} A/cm^2. Thus, we have a very sensitive test for trace oxidizable impurities. Furthermore, the oxygen (or reducible) impurity level is at least an order of magnitude less. This will be discussed further in the next section.

In the Tafel region with a 0.12 slope (Fig. 1), an oxidation reaction is occurring which undoubtedly involves water. The formation of atomic oxygen is unlikely since no hysteresis effects are noted if the potential remains below 1 volt. The 0.12 slope indicates a one-electron slow discharge. Some authors (12) have postulated the formation of the hydroxyl radical

$$Pt + H_2O \rightarrow H^+ + Pt\text{-}OH + e. \qquad (1)$$

At a steady-state condition the level of OH adsorption is maintained constant by OH possibly decomposing to water and O_2. The data in Fig. 1 strongly supports such a mechanism—however, it does not prove it. The data in Figs. 2(a) and (b), which show the effects of diffusion control, give essentially the same Tafel slopes. We have no ready explanation of this.

In the potential range from 1.0 to 1.1 volts (Fig. 1) a Tafel slope of 0.13 is found only when potentials above ~1.4 volts do not precede this range. Here, again, the slope indicates a one-electron rate-controlling mechanism. At these potentials, previous experience at this and other laboratories indicates the formation of O atoms. The mechanism could be

$$Pt\text{-}OH \rightarrow Pt\text{-}O + H^+ + e. \qquad (2)$$

Under steady-state conditions, the amount of O associated with the Pt would be constant, the excess O being lost possibly by peroxide formation and decomposition. The atomic oxygen can be both dermasorbed in the skin of the Pt and be chemisorbed on the surface. In the 1.0- to 1.1-volt range represented by the 0.13 slope, dermasorption most likely occurs to only a small extent. This is indicated by going to a more anodic potential of 1.4 volts and then decreasing the potential (◊) points with no apparent deviation. The limiting current at about 3×10^{-6} A/cm^2 appears to be on Pt fully covered with O_{ad}, with only small absorption of O atoms. The surface coverage with atomic oxygen probably varies in the first 0.13 slope range, but full coverage is obtained at values above 1.1 volts. Only when the potential rises to about 1.7 volts is there an indication that molecular oxygen is evolved in quantity and that saturation of the dermalayer is complete. This is shown both by the lower current densities on the decreasing potential curve and the fact that, after reaching a potential of about 0.9 volt, a subsequent increase in potential to 1.36 volts will give a current density (♦ , Fig. 1) somewhere between the two branches of the hysteresis loop. The degree of oxygen saturation of the dermalayer thereby appears to be both a function of potential and previous history.

The atomic oxygen formation region (1.0 to 1.7 volts) appears to give off a diffusable produce as is evident from the effects of diffusion currents obtained in Figs. 2(a) and (b). Whether this product is O_2, H_2O_2, or something else is not obvious, although the rate of diffusion does generally follow the same potential independence seen for the kinetic reaction in Fig. 1. This is reasonable since the limiting current densities show that the rates of formation of products are independent of potential. This indicates that dermasorption of

O atoms could be rate-controlling. At potentials above ~1.6 volts, the current density is independent of stirring rate. This shows that the rate-determining step in the oxygen gas formation reaction is so slow that it gives complete kinetic control, and that diffusion away of molecular oxygen contributes nothing to the overvoltage.

The potential region above 1.6 volts is undoubtedly the molecular oxygen generation region, where the Tafel slope of 0.13 again indicates a rate-controlling step involving a one-electron reaction. This slope verifies Hoare's work (13). The total oxygen generating mechanism may be

$$\begin{aligned} &Pt + H_2O \rightarrow Pt\text{-}OH + H^+ + e \\ &Pt\text{-}OH \rightarrow Pt\text{-}O + H^+ + e \\ &\left.\begin{aligned} &Pt\text{-}O + H_2O \rightarrow Pt + H_2O_2 \\ &H_2O_2 \rightarrow H_2O + 1/2\ O_2 \end{aligned}\right\} \quad (\text{or, } 2Pt\text{-}O \rightarrow 2Pt + O_2). \end{aligned} \tag{3}$$

Under these conditions the Pt skin is saturated with dermasorbed O atoms and the current densities are independent of increasing or decreasing potentials.

After the electrode had been taken to potentials above 1.7 volts, upon decreasing the potential to about 0.9 volt, the transient anodic current density decreased and eventually became cathodic. Under these conditions, increasing the rate of He flow decreased the net cathodic current density. This can be explained by the fact that the anodic current increases with increased stirring rate [Fig. 2(b)]. Thus the increased rate of the anodic reaction plus the cathodic reaction gave a lower net cathodic current. This cathodic current persisted for about two days and eventually returned to the anodic current indicated in Fig. 1 at this potential. These decreases in anodic current were undoubtedly due to the oxygen, stored primarily in the dermalayer, migrating to the surface and being reduced to water. The fact that increased He stirring appears to increase the rate of the anodic reaction with little change in the rate of the cathodic reaction bears this out. This further indicates that dermasorbed oxygen is unstable at potentials below 1 volt, and even though the small hysteresis effects found at potentials below 1 volt are probably due to small traces of dermasorbed O, the bulk of these dermasorbed O atoms is removed. It is quite possible that at potentials below 1 volt at least part of the source of dermasorbed O is from the interior of the metal and this migration is so slow that its removal takes some time. Once the electrode is taken into the cathodic current region and held there for some hours, the potential vs current behavior over the entire anodic current range is essentially the same as shown for the potential increasing values shown in Fig. 1.

Impurity Levels in Solution

One of the goals of this investigation was to determine quantitatively the maximum levels of impurities in the solution. As mentioned above, the data in Fig. 1 indicated that the level of impurities which were reducible in the vicinity of 0.46 volt were below an amount which would give a cathodic current of -10^{-9} A/cm^2 on the Pt bead electrode. This was determined by the lack of stirring effects in this region. It also was shown that the maximum amount of oxidizable impurity in the vicinity of 0.49 volt gave an equivalent of about 2×10^{-9} A/cm^2. These current densities give upper limits of the amounts of both oxidizable and reducible impurities which actually react at the working electrode surface.

Since, as will be shown, the level of reducible impurity (most likely O_2) in solution is at least one order of magnitude less than oxidizable impurities (H_2 and organic species), reducible impurities will have an insignificant effect on the anodic current density due to

oxidizable impurities. Similarly, at cathodic current densities of -10^{-9} A/cm^2, and at anodic current densities of 10^{-8} A/cm^2, there are negligible impurity effects. To give some idea of how low these impurity levels are, the fraction of Pt surface which reducible impurities (mostly O atoms) contact in one second must be less than 2×10^{-6}, and the fraction of Pt surface which H atoms (or equivalent organic molecules) contact in one second must be not more than 4×10^{-5}. Of course, this tells us nothing about the catalytic effects of these very small amounts of impurities. However, the data which will be given next on the effects of additions of trace amounts of hydrogen and oxygen indicate that, at these low impurity levels, increased, but still very small, amounts of these impurities have no apparent catalytic effects.

Because of the very low net currents involved, the potential region from 0.46 to 0.50 volt is most sensitive to added impurities. By controlling the potential at 0.46 volt, the effects of trace amounts of hydrogen and oxygen* on the original net cathodic current is seen in Fig. 3. Controlling the potential at 0.50 volt gave the data shown in Figs. 4 and 5.

The data in Fig. 3 shows that when successive small amounts of either hydrogen or oxygen are added to the helium gas stream to give the partial pressures shown, a detectable change in the cathodic current density is felt between 10^{-7} and 10^{-6} atm of H_2 or O_2. An estimate of the diffusion current that would result if all of the hydrogen or oxygen which reached the surface reacted can be obtained from the Nernst diffusion equation (14)

$$i_{diff} = 1/2j = \frac{DF\,(C_o - C_s)}{2 \times 10^3\,\delta} \tag{4}$$

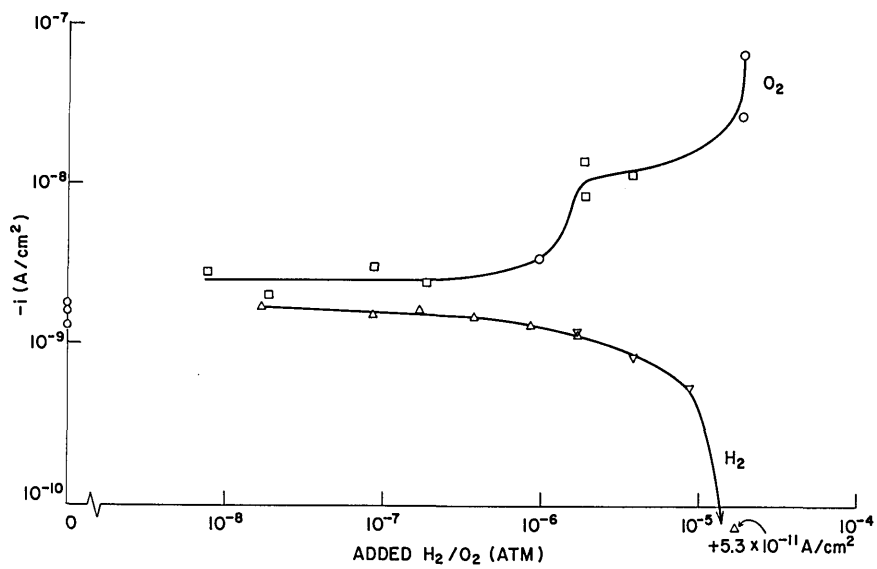

Fig. 3 - Changes in net cathodic current density Δi at 0.46 volt vs added H_2 and O_2 for a helium flow rate of 40 ml/min. Curves are labeled: △ added H_2, increasing partial pressures; ▽ added H_2, decreasing partial pressures; o added O_2, increasing partial pressures; and □ added O_2, decreasing partial pressures.

*See Ref. 15 for technique used for additions of small partial pressures of hydrogen and oxygen to helium carrier gas.

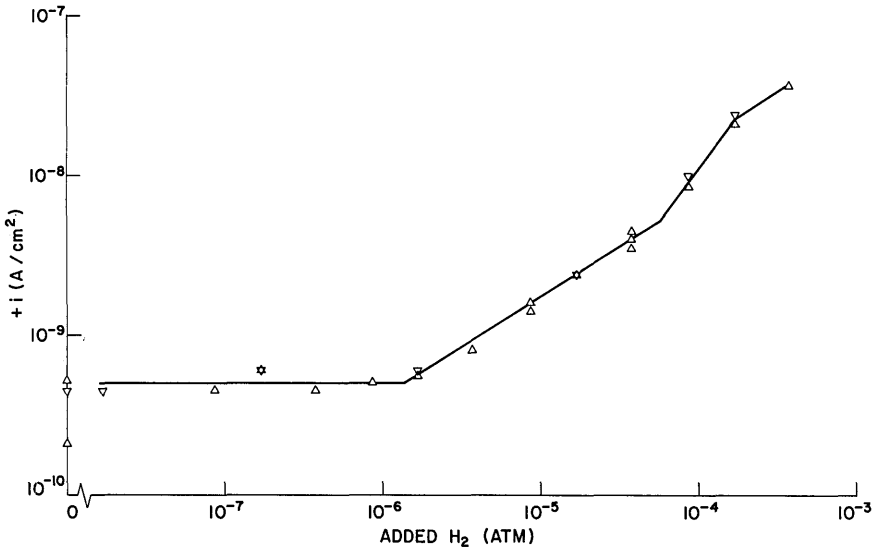

Fig. 4 - Increases in the net anodic current density at 0.50 volt vs added H_2 for a helium flow rate of 40 ml/min. Symbols are the same as in Fig. 3.

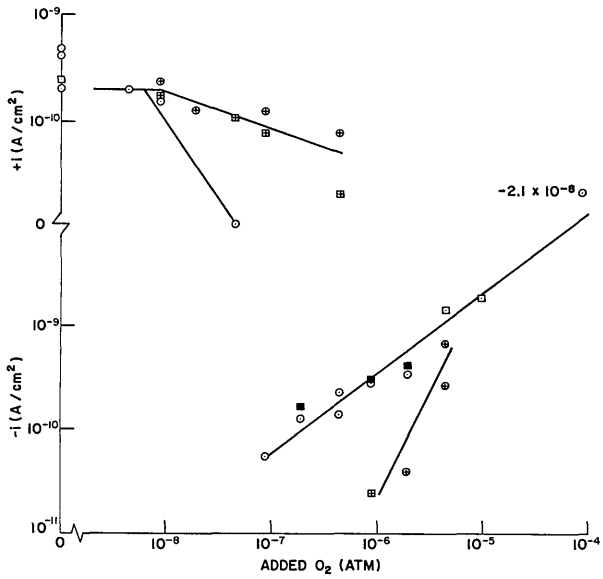

Fig. 5 - Decreases in the net anodic current density and transition to net cathodic current density at 0.50 volt vs added O_2 for a helium flow rate of 40 ml/min. Curves are labeled: ⊙ first run, increasing O_2 partial pressure; ⊡ first run, decreasing O_2 partial pressure; ⊕ second run, increasing O_2 partial pressure; ⊞ second run, decreasing O_2 partial pressure; and ■ third run, decreasing O_2 partial pressure.

where j* is the calculated diffusion current density in A/cm^2, D is the diffusion coefficient, F is the faraday, C_o is the concentration of the additive in the bulk of the solution in equiv/l, C_s is the concentration at the surface, which is zero at steady state, and δ is the "effective thickness" of the boundary layer.

The current due to diffusion of dissolved gases to the electrode may be calculated using $D_{H_2} = 4.87 \times 10^{-5}$ cm^2/sec (16), and $D_{O_2} = 1.98 \times 10^{-5}$ cm^2/sec (16). Thus,

$$(C_o)_{H_2} = \frac{0.0149 \times 1000 \times 2}{22{,}400} P_{H_2} = 1.33 \times 10^{-3} P_{H_2} \text{ equiv H/l}$$

$$(C_o)_{O_2} = \frac{0.023 \times 1000 \times 4}{22{,}400} P_{O_2} = 4.1 \times 10^{-3} P_{O_2} \text{ equiv O/l} \tag{5}$$

where 0.0149 and 0.023 are the respective Bunsen coefficients (standard cc gas in 1 cc of 1M H_2SO_4 (17)) of H_2 and O_2, respectively, 2 and 4 are the respective number of electrons involved in H_2 oxidation and O_2 reduction, and P is the partial pressure of each gas in atm. Thus,

$$i_{diff,\ H_2} = 3.25 \times 10^{-6} \frac{P_{H_2}}{\delta} \quad (A/cm^2)$$

$$i_{diff,\ O_2} = -4.06 \times 10^{-6} \frac{P_{O_2}}{\delta} \quad (A/cm^2). \tag{6}$$

Since the changes in current densities found in Figs. 3, 4, and 5, upon addition of either hydrogen or oxygen, are due to their respective oxidation or reduction, and assuming that the changes in current are primarily due to the rate of diffusion of these gases to the surface, we can calculate

$$i_{res} = i_{meas} - i_{diff}. \tag{7}$$

In Eq. (7), i_{res} is the residual current density in the absence of added hydrogen or oxygen, i_{meas} is the measured current density found in the presence of added hydrogen or oxygen and is taken from Figs. 3, 4, and 5, and i_{diff} is the diffusion current calculated from Eq. (6). The value of δ was adjusted to give the most constant i_{res} values. This gave a δ value of 0.035 cm for H_2 and a value of 0.02 cm for O_2. These were reasonable values when compared to the data of Ibl (18) for a δ in moderately stirred solution (helium flow of 40 ml/min). Using these values of δ and Eqs. (6) and (7), the results shown in Table 1 were obtained.

The data in block (a) of Table 1 shows that, at 0.46 volt, changes in the partial pressure of hydrogen give a constant i_{res} which is very close to the value found in the absence of added hydrogen. Hence current changes due to hydrogen at this potential are essentially diffusion-controlled. The data in block (b) of Table 1, taken at 0.50 volt, also shows hydrogen diffusion control. At P_{H_2} values above 1×10^{-4} atm a kinetic process is involved since the calculated diffusion current density does not account for all of the current density increase. For some reason, at partial pressures above 10^{-4} atm, the rate of the oxidation

*To put i_{diff} on a true area basis, the roughness factor of the electrode being ~2, j in Eq. (4) is divided by 2.

Table 1
Effects of Added H_2 and O_2 on the Residual Current Density i_{res}

(a) at 0.46 volt			(b) at 0.50 volt		
P_{H_2} (atm)	$i_{meas} \times 10^9$ (A/cm²)	$i_{res} \times 10^9$ $\delta = 0.035$ cm (A/cm²)	P_{H_2} (atm)	$i_{meas} \times 10^{10}$ (A/cm²)	$i_{res} \times 10^{10}$ $\delta = 0.035$ cm (A/cm²)
5×10^{-8}	-1.6	-1.6	1×10^{-7}	5	4.9
1×10^{-7}	-1.5	-1.5	1×10^{-6}	5	4.1
5×10^{-7}	-1.4	-1.4	1×10^{-5}	17	7.7
1×10^{-6}	-1.3	-1.4	2×10^{-5}	27	9.4
5×10^{-6}	-0.76	-1.2	1×10^{-4}	100	7.0
1×10^{-5}	-0.40	-1.3	2×10^{-4}	250	64.0
			3.5×10^{-4}	360	34.0
i_{res} at $P_{H_2} = 0$ (Fig. 3) is -1.3 to -1.8			i_{res} at $P_{H_2} = 0$ (Fig. 4) is 2 to 5		

(c) at 0.46 volt			(d) at 0.50 volt		
P_{O_2} (atm)	$i_{meas} \times 10^9$ (A/cm²)	$i_{res} \times 10^9$ $\delta = 0.02$ cm (A/cm²)	P_{O_2} (atm)	$i_{meas} \times 10^{10}$ (A/cm²)	$i_{res} \times 10^{10}$ $\delta = 0.02$ cm (A/cm²)
5×10^{-8}	-2.5	-2.5	$*5 \times 10^{-9}$	2	2
1×10^{-7}	-2.5	-2.5	$*1 \times 10^{-8}$	1	2
5×10^{-7}	-4.0	-4.0	$*1 \times 10^{-7}$	-0.6	-0.4
1×10^{-6}	-6.0	-5.8	$*1 \times 10^{-6}$	-3.6	-1.6
5×10^{-6}	-14	-13	$*1 \times 10^{-5}$	-20	0
1×10^{-5}	-25	-23	$\dagger 5 \times 10^{-9}$	2	2
			$\dagger 1 \times 10^{-8}$	2	2
			$\dagger 1 \times 10^{-7}$	0.9	0.7
			$\dagger 1 \times 10^{-6}$	-0.2	1.9
			$\dagger 1 \times 10^{-5}$	-20	0
i_{res} at $P_{O_2} = 0$ (Fig. 3) is -1.3 to -1.8			i_{res} at $P_{O_2} = 0$ (Fig. 5) is 2 to 5		

*See Fig. 5, curves ⊙, ⊡, and ■.
†See Fig. 5, curves ⊕ and ⊞.

reaction on the surface increases. This may be due to changes in the catalytic properties of the surface.

The data in blocks (c) and (d) of Table 1 concerning the effects of oxygen additions, however, cannot be simply attributed to diffusion control. At 0.46 and at 0.50 volt, up to 1×10^{-6} atm of added O_2 essentially shows $i_{res} \approx i_{meas}$. This means that i_{diff} is relatively insignificant. Even though the scatter at 0.50 volt is not too satisfactory, diffusion control is apparently unimportant except at $P_{O_2} \geq 10^{-6}$ atm. Since changes in the measured current density were rather small, the oxygen reduction reaction is relatively slow, and even though real effects of added oxygen are apparent in Fig. 5, they are very small.

At 0.46 volt the i_{res} values are not constant at partial pressures above 1×10^{-7} atm of added oxygen; also, the residual current densities are essentially equal to the measured current densities. Diffusion control is evidently a minor factor. It appears that the oxygen which gets to the surface effectively increases the rate of the hydrogen formation reaction. This appears to be a catalytic effect and may be attributed to the removal of catalytic poisons from the electrode surface by chemical oxidation. These poisons may be trace amounts of organic species, or even hydrogen itself.

Even with the scatter found for different runs, it is obvious that oxygen additions as low as 10^{-8} atm significantly decrease the net anodic current density. This specifically shows that the oxygen impurity must be at least an order of magnitude less than 10^{-8} atm and confirms previous estimates (1) of oxygen impurity in our closed system. Since, at 10^{-8} atm, O_2 diffusion will give an i_{diff}, O_2 of about -2×10^{-12} A/cm^2, and the actual current density found at O_2 additions of 10^{-8} atm (Fig. 5) is between $+1 \times 10^{-10}$ and $+2 \times 10^{-10}$ A/cm^2, O_2 is only cancelling out a small part of the oxidizable impurity which must be an amount required to give an equivalent of about 10^{-10} A/cm^2. Since the current density attributable to oxidizing impurities at 0.49 volt was about an order of magnitude more, we can conclude from this and the abnormally high effect of O_2 additions that oxygen is affecting the net anodic current density as a catalytic poison.

The sensitivity of this technique of determining maximum possible anodic and cathodic impurity levels and of the purity of the system used can be better demonstrated if the impurity effects are expressed in normal analytical terms of parts per million (gm of H_2 or O_2 per gm solution). The conversion factors are

$$(2 \times 0.0149/22,400 \times 1.06)P_{H_2} = 1.25 \times 10^{-6}\ P_{H_2}\ \text{(gm } H_2 \text{ per gm 1M } H_2SO_4)$$

and

$$(32 \times 0.023/22,400 \times 1.06)P_{O_2} = 3.1 \times 10^{-5}\ P_{O_2}\ \text{(gm } O_2 \text{ per gm 1M } H_2SO_4),$$

where P_{H_2} and P_{O_2} are the gas partial pressures in atm, 2 and 32 are the respective molecular weights of H_2 and O_2, 0.014 and 0.023 are the Bunsen coefficients of H_2 and O_2 (17), respectively, 22,400 is the number of cc of gas in one mole equivalent, and 1.06 is the specific gravity of 1M H_2SO_4. Thus the detection sensitivity is 10^{-7} ppm for O_2 and 10^{-6} ppm for H_2. Since oxidizable impurities could be partly organic species, the level of this impurity could be considerably less on a molecular basis, but would have to be more on a weight basis. The actual impurity levels in solution are easily an order of magnitude less than the maximum impurity levels determined.

The really critical impurity level, from an electrochemical viewpoint, would concern the fraction of available Pt sites covered with impurity. Here again, from the data shown in Fig. 1, we have seen that reducible impurities which get to the surface give a current density which must be less than -1×10^{-9} A/cm^2, and oxidizable impurities give a current density of not more than 2×10^{-9} A/cm^2. This means that less than 10^9 electrons are

used in reducible impurities per cm^2 per sec and not more that 10^{10} electrons are donated by oxidizable impurities per cm^2 per sec. Since the total number of Pt atoms per cm^2 is about 1.3×10^{15}, then in one second, less than one available Pt surface site per million can be affected by reducing impurity reaction and less than one available Pt surface site per 100,000 can be affected by an oxidizing impurity reaction.

CONCLUSIONS

1. In the potential range from 0.06 to 0.13 volt, under rapid stirring with helium, the reaction mechanism rate-controlling step is

$$Pt\text{-}H + H^+ + e = H_2.$$

The net increased diffusion of H_2 away from the surface by rapid stirring can be determined by subtracting the current density under slow stirring from the current density under fast stirring. This indicated that the Tafel component due to increased diffusion gave a slope of -0.03. However, at slow stirring rates, diffusion and kinetic control were about equal.

2. A second Tafel region between 0.30 to 0.46 volt indicated a slow hydrogen-ion discharge step.

3. The potential at which no net reduction or oxidation reaction occurs (transition point from net cathodic to net anodic reaction) and at which H and O adsorption is equal to zero is about 0.46 volt relative to a normal hydrogen electrode (NHE).

4. Four distinct Tafel regions were found in the anodic range from 0.46 to >2 volts. These were: a region in which oxidizable impurities reacted; a region at which water was probably oxidized to give chemisorbed OH; a region in which chemisorbed and dermasorbed O was formed; and a region in which O_2 was generated.

5. A hysteresis effect was found, once significant amounts of O were dermasorbed. This lowered the net reaction rates.

6. Impurity levels both in solution and on the electrode surface were determined. The maximum possible level of reducible impurity was found to be equivalent to an O_2 concentration of 10^{-7} ppm and a maximum oxidizable impurity level equivalent to an H_2 concentration of 10^{-6} ppm. The impurity levels of oxidizable and reducible species on the Pt surface were less than equivalent to 10^{10} and 10^9 electrons per cm^2 per sec, respectively. This means that about one available Pt surface site per million per sec is affected by an impurity reaction. In a 10^{-12} torr vacuum system, N_2 arrives at a surface at a rate of about 4×10^8 molecules per cm^2 per sec (19). The rate of electrode contamination in our system is comparable.

7. Very small additions of hydrogen or oxygen in the critical transition region from net cathodic to net anodic reaction did not have catalytic effects, but when the partial pressure of these gases was above 10^{-6} atm catalytic effects were apparent.

8. Further experimental work is required using transient measurements in conjunction with potentiostatic control to determine the kinetic parameters in each of the Tafel regions to determine surface and dermasorbed layer coverages and other kinetic parameters.

9. This study has demonstrated that highly purified, closed, electrochemical systems can give precise information concerning voltage regions at which net reaction rates are very slow.

REFERENCES

1. Schuldiner, S., Piersma, B.J., and Warner, T.B., J. Electrochem. Soc. 113:573 (1966)
2. Schuldiner, S., and Roe, R.M., J. Electrochem. Soc. 110:332 (1963)
3. Schuldiner, S., and Roe, R.M., J. Electrochem. Soc. 110:1142 (1963)
4. Schuldiner, S., Castellan, G.W., and Hoare, J.P., J. Chem. Phys. 28:16 (1958)
5. Schuldiner, S., and Warner, T.B., J. Phys. Chem. 68:1223 (1964)
6. Kandler, L., Knorr, C.A., and Schwitzer, C., Z. Physik, Chem. A180:281 (1937)
7. Knorr, C.A., Z. Elektrochem. 59:647 (1955)
8. Schuldiner, S., J. Electrochem. Soc. 108:384 (1961)
9. Horiuti, J., and Polyani, M., Acta Physicochim. (USSR) 2:505 (1935)
10. Parsons, R., Trans. Faraday Soc. 54:1053 (1958)
11. Gerischer, H., Bull. Soc. Chim. Belg. 67:506 (1958)
12. Bockris, J.O'M., J. Chem. Phys. 24:817 (1956); H. Wroblowa, B.J. Piersma and J.O'M. Bockris, J. Electroanal. Chem. 6:401 (1963); J.P. Hoare, J. Electrochem. Soc. 112:602 (1965)
13. Hoare, J.P., Electrochim. Acta 11:203 (1966)
14. King, C.V., J. Electrochem. Soc. 102:193 (1955)
15. Warner, T.B., and Schuldiner, S., J. Electrochem. Soc. 112:853 (1965)
16. Conway, B.E., "Electrochemical Data," p. 174, Amsterdam:Elsevier Publ. Co., 1952
17. "International Critical Tables," 3:271 (1928)
18. Ibl, N., Chem.-Ing.-Tech. 33:69 (1961)
19. Ehrlich, G., "Advances in Catalysis," Vol. 14, p. 392, New York:Academic Press, 1963

Security Classification

DOCUMENT CONTROL DATA - R & D

(Security classification of title, body of abstract and indexing annotation must be entered when the overall report is classified)

1. ORIGINATING ACTIVITY *(Corporate author)* Naval Research Laboratory Washington, D.C. 20390	2a. REPORT SECURITY CLASSIFICATION Unclassified 2b. GROUP

3. REPORT TITLE

POTENTIOSTATIC CURRENT-POTENTIAL MEASUREMENTS ON A PLATINUM ELECTRODE IN A HIGH-PURITY CLOSED SYSTEM

4. DESCRIPTIVE NOTES *(Type of report and inclusive dates)*

An interim report; work on the problem continues.

5. AUTHOR(S) *(First name, middle initial, last name)*

S. Schuldiner, T.B. Warner, and B.J. Piersma

6. REPORT DATE March 6, 1967	7a. TOTAL NO. OF PAGES 18	7b. NO. OF REFS 19
8a. CONTRACT OR GRANT NO. NRL Problem C05-13 b. PROJECT NO. RR 001-01-43-4754 c. d.	9a. ORIGINATOR'S REPORT NUMBER(S) NRL Report 6504 9b. OTHER REPORT NO(S) *(Any other numbers that may be assigned this report)* None	

10. DISTRIBUTION STATEMENT

Distribution of this document is unlimited.

11. SUPPLEMENTARY NOTES None	12. SPONSORING MILITARY ACTIVITY Dept. of the Navy (Office of Naval Research)

13. ABSTRACT

In a high-purity, closed, electrochemical system, voltage regions at which very slow reactions are rate-controlling, were accurately separated and measured. In the potential range from 0.06 to 0.13 volt, the rate-controlling step is $Pt\text{-}H + H^+ + e = H_2$ under conditions of rapid stirring with helium. A second region between 0.30 and 0.46 volt indicated a slow hydrogen-ion discharge. In the anodic range from 0.46 to >2 volts, four distinct regions were found: a region in which oxidizable impurities reacted; a region at which water was probably oxidized to give chemisorbed OH; a region in which chemisorbed and dermasorbed O was formed; and a region in which O_2 was generated.

Maximum oxidizable and reducible impurity levels were quantitatively determined both in solution and as adsorbed species on the working electrode surface. It is shown that the impurity levels were very low. Very small additions of hydrogen or oxygen in the critical transition region (net cathodic to anodic reactions) did not appear to have catalytic effects. However, at oxygen partial pressures above 10^{-7} atm, a poisoning effect was apparent.

DD FORM 1 NOV 65 1473 (PAGE 1)

S/N 0101-807-6801

Security Classification

14. KEY WORDS	LINK A ROLE	LINK A WT	LINK B ROLE	LINK B WT	LINK C ROLE	LINK C WT
Electrodes						
Platinum						
Electrochemistry						
Voltage						
Electric Currents						
Dermasorption						
Reaction Kinetics						
Impurities						
Adsorption						
Oxidation						
Oxidation-Reduction Reactions						
Analysis						
Catalysts						
Fuel Cells						